Synchronous Generator Model Identification and Parameter Estimation From Operating Data

H. Bora Karayaka, Ali Keyhani, *Fellow, IEEE*, Gerald Thomas Heydt, *Fellow, IEEE*, Baj L. Agrawal, *Fellow, IEEE*, and Douglas A. Selin, *Senior Member, IEEE*

***Abstract*—A novel technique to estimate and model parameters of a 460-MVA large steam turbine generator from operating data is presented. First, data from small excitation disturbances are used to estimate linear model armature circuit and field winding parameters of the machine. Subsequently, for each set of steady state operating data, saturable inductances L_{ds} and L_{qs} are identified and modeled using nonlinear mapping functions-based estimators. Using the estimates of the armature circuit parameters, for each set of disturbance data collected at different operating conditions, the rotor body parameters of the generator are estimated using an output error method (OEM). The developed nonlinear models are validated with measurements not used in the estimation procedure.**

***Index Terms*—Armature circuit and rotor body parameters, large utility generators, parameter identification.**

I. Introduction

PARAMETER identification from operating data for synchronous generators is a beneficial procedure which does not require any service interruption to perform. Thus, machine parameters, which can deviate substantially from manufacturer values during online operation at different loading levels, can be determined without costly testing [1]. These deviations are usually due to magnetic saturation [2]–[4], internal temperature, machine aging, and the effect of centrifugal forces on winding contacts and incipient faults within the machine. References [5]–[7] include investigations into modeling synchronous generator parameters as a function of operating condition. In most of these studies, the independent variables used in modeling nonlinear variations of the parameters are primarily the terminal voltage, current, or a combination of these quantities including the phase angle. A similar study can be found in [7] and [8] for a small round rotor synchronous generator.

In this study, disturbance data sets acquired online at different loading and excitation levels of a large utility generator are used to identify the machine parameters. It is assumed that the machine model order is known (i.e., the number of differential equations). Estimated machine parameters for each operating point are then mapped into operating condition-dependent machine variables using nonlinear mapping functions. The nonlinear mapping [7] can easily identify the shape of the nonlinear function from training data. Therefore, no *apriori* knowledge of the shape of the mapping is required. The effects of generator saturation, rotor position, and loading are included in the mapping process. Finally, validation studies are conducted to investigate the performance of nonlinear mapping models and estimated parameters.

Manuscript received July 17, 2000; revised October 26, 2001. This work is supported in part by the National Science Foundation, Grant ECS9722844.

H. B. Karayaka and A. Keyhani are with Department of Electrical Engineering, Ohio State University, Columbus, OH 43210 USA

G. T. Heydt is with Arizona State University, Tempe, AZ 85287 USA

B. Agrawal and D. Selin are with Arizona Public Service Company, Phoenix, AZ 85062 USA

Digital Object Identifier 10.1109/TEC.2002.808347

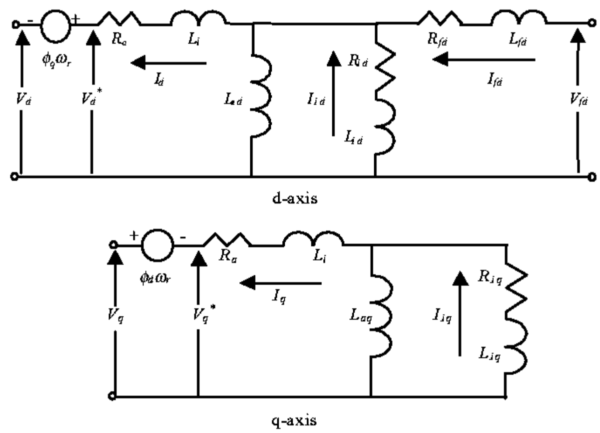

Fig. 1. Online model structure.

II. Machine Model Description and Problem Formulation

The structure of the synchronous machine model used in this study is a *model 2.1.* type [1], with one damper in the d*-axis* and one damper in the q*-axis*, given in Fig. 1.

For continuous time systems, the state space representation of this model is

$$\begin{aligned}\frac{dX(t)}{dt} &= A(\theta)\cdot X(t) + B(\theta)\cdot U(t) + w(t)\\ Y(t) &= C\cdot X(t) + v(t)\end{aligned} \tag{1}$$

where $w(t)$ and $v(t)$ represent the process and measurement noise. Also, see the equation at the bottom of the next page. All parameters are in actual units. Also, it is assumed that the machine power angle δ is available for measurement. Variables v_d, v_q, i_d, and i_q represent generator d- and q*-axis* terminal voltages and currents, respectively. The quantities i_{fd}^* and v_{fd}^* represent field current and field voltage, respectively, as measured on the field side of the generator and R_{fd}^* is the field winding resistance as measured on the field side. Terms i_{fd}, v_{fd}, and R_{fd} represent corresponding transformed quantities on the stator side through the field to stator turns ratio $a = N_{fd}/N_s$ as follows:

$$i_{fd} = \frac{2}{3} a i_{fd}^* \quad v_{fd} = \frac{v_{fd}^*}{a} \quad R_{fd} = \frac{3}{2}\frac{1}{a^2} R_{fd}^*.$$

All other variables and parameters are referred to the stator.

The identification of machine parameters including armature, field, and rotor body parameters involve the following five stages.

1) Measurement data are validated.
2) Using small excitation disturbance data, linear model armature circuit and field winding parameters are estimated.
3) Saturable inductances L_{ds} and L_{qs} are identified for each steady-state operating point and nonlinear models are developed for mapping L_{ds} and L_{qs} to various operating points.
4) Using the armature circuit parameter estimates from the previous step, rotor body parameters are estimated from disturbance data acquired when the machine is operating online under various test conditions.
5) Nonlinear mapping models are developed and validated to map variables representative of generator operating condition to each rotor body parameter.

Stage 1 is discussed in detail in a recent study by the authors [18]. Stages 2—5 comprise the primary objectives of this paper. In order to validate the established model based on estimated parameters, simulation studies are also performed and the results are compared against the simulation results with manufacturer parameters. In these studies, measured terminal and field voltages are used to excite the machine model to obtain terminal and field currents. The simulated currents are compared against corresponding actual measurements.

The large steam generator used for study purposes is one of the Cholla Units operated by Arizona Public Service Co. (APS). This machine is rated at 22 kV, 460 MVA, and operates at 3600 r/min. The generator is monitored continuously, and data are recorded at an operator's demand or when a fault condition occurs. The data consist of measurements of stator voltages and currents, field voltage and current, generator speed, and power angle. Ten steady-state data files at various operating conditions were used in this paper's analysis. Thirteen transient data files were obtained either by stepping the voltage regulator for short periods of time or by capturing fault conditions.

III. Estimation of Linear Model Armature Circuit and Field Winding Parameters

The first stage of the estimation process involves estimation of linear model armature circuit and field winding parameters of the machine. In order to satisfy linearity, the field side of the machine should be disturbed in small amounts (approximatelyt 5 to 10%) while the machine is underexcited and operating at light load. The measurements needed for the estimation process are v_{ab}, v_{bc}, v_{ca}, i_{as}, i_{bs}, i_{cs}, i_{fd}^*, and δ. These quantities can be converted to dq-axis equivalents by following the steps described in reference [20].

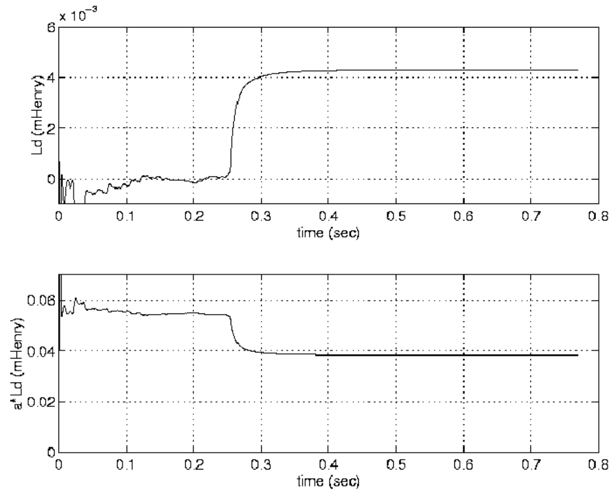

Fig. 2. Recursively estimated aL_{ad} and L_d trajectories.

A recursive estimation procedure [20] is used to estimate the armature circuit parameters R_a, aL_{ad}, and L_d from two different small disturbance data. Due to the sensitivity of estimation of L_q to the accuracy of δ for small angles [18], it was not feasible to estimate L_q for these operating points. The trajectories of recursively estimated aL_{ad} and L_d are given in Fig. 2. In addition to the armature circuit parameters, field winding parameters R_{fd}^* and L_{fd} are also estimated, applying output error method (OEM) technique [21] to these small disturbance data sets in that the contribution of damper winding effects can be ignored. Table I lists the estimated parameters for these two cases. Although the machine can be assumed to be linear while it is underexcited, there is still a slight difference between estimated parameters for two different operating conditions.

Due to the sensitivity of aL_{ad}, L_d, R_{fd}^*, and L_{fd}, estimates are quite negligible even for significant changes in R_a as shown in Table I, the value of R_a can be set as the manufacturer's value 0.0047 Ω. Also, the leakage inductance L_l is assumed to be 10% of L_d, as given by manufacturer-supplied values. Based on this value of L_l, the value of turns ratio a was found to be within the range of 9.9. This tuning procedure is obtained by experience with the measured and manufacturer's data and confidence in their values.

$$\begin{aligned}
X &= [\, i_q \quad i_d \quad i_{1q} \quad i_{1d} \quad i_{fd}^* \,]^T \\
U &= [\, v_q \quad v_d \quad v_{fd}^* \,]^T \\
Y &= [\, i_q \quad i_d \quad i_{fd}^* \,]^T \\
\theta &= [\, R_a \quad R_{fd}^* \quad R_{1d} \quad L_l \quad L_{ad} \quad L_{fd} \quad L_{1d} \quad a \quad R_{1q} \quad L_{aq} \quad L_{1q} \,]^T
\end{aligned}$$

TABLE I
ARMATURE RESISTANCE SENSITIVITY ANALYSIS ON ESTIMATION WITH SMALL DISTURBANCE DATA

	Ra (Ω)	Ld (mH)	a*Lad (mH)	Rfd (Ω)	Lfd (mH)
Small Disturbance Case #1	0.0024	4.2224	37.466	0.0459	0.3506
	0.0047	4.2222	37.466	0.0465	0.3359
	0.0095	4.2219	37.466	0.0472	0.3228
Small Disturbance Case #2	0.0024	4.2714	38.386	0.0524	0.3225
	0.0047	4.2714	38.386	0.0523	0.3185
	0.0095	4.2714	38.386	0.0522	0.3120

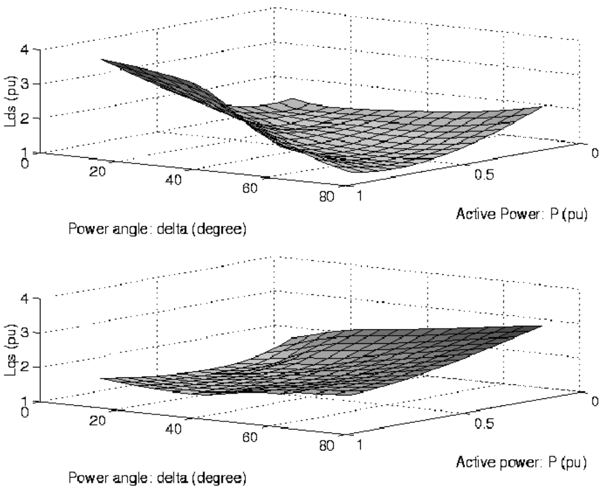

Fig. 3. Variation of L_{ds} and L_{qs} as a function of power angle (δ) and active power (P).

IV. DEVELOPMENT OF SATURATION MODELS

First, saturable inductances L_{ds} and L_{qs} are identified from each steady-state operating data collected at various levels of excitation and power generation. Since R_a, L_l, and a are already determined in the previous stage, L_{ds} and L_{qs} can be calculated for each steady-state operating point using the following equations:

$$L_{ds} = \frac{v_q + R_a \cdot i_q}{-\omega \cdot i_d + \frac{2}{3} \cdot a \cdot \omega_r \cdot i_{fd}^* \cdot 0.9} \tag{2}$$

$$L_{qs} = \frac{v_d + R_a \cdot i_d}{\omega \cdot i_q}. \tag{3}$$

A total of 34 steady-state data points were used to identify L_{ds} and 29 of which (excluding operating points with small δ. angles) were used to identify L_{ds}. Fig. 3 depicts the variation of L_{qs} and L_{ds} as a function of power angle and active power at the machine-rated terminal voltage for these data points.

Once the inductance values are identified for each operating point, the nonlinear mapping saturation models can be developed. The nonlinear mapping function to be identified between the input and output patterns is proposed as

$$\begin{cases} L_{ds} = & N_d\,(v_d \quad v_q \quad i_d \quad i_q \quad i_{fd}^*) \\ L_{qs} = & N_q\,(v_d \quad v_q \quad i_d \quad i_q \quad i_{fd}^*) \end{cases} \tag{4}$$

where N_d and N_q are unknown nonlinear mapping functions to be established. The field voltage v_{fd}^* need not be a part of the mapping since it is simply a scaled version of field current i_{fd}^* at steady state.

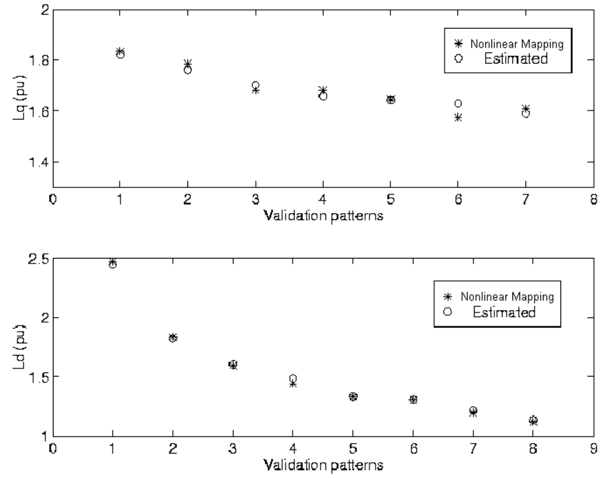

Fig. 4. Nonlinear mapping and OEM estimated L_{ds} and L_{qs} for the patterns not used in training.

In order to verify that the nonlinear mapping functions are able to generalize properly, a cross validation data set, which is not included in the estimation, is used after the model development. The values of estimated L_{ds} and L_{qs} are compared with the cross validation set not previously used for modeling. As shown in Fig. 4, both nonlinear functions saturation models can correctly interpolate between patterns not used in estimation.

V. ESTIMATION OF ROTOR BODY PARAMETERS

The estimation procedure involves the identification of field winding d- and q-axis damper winding parameters from disturbance data. For estimation of rotor body parameters, operating data due to disturbances that will excite adequate amount of damper winding currents are needed. For instance, this can be achieved by perturbing the field excitation voltage or by capturing line fault events.

The armature circuit parameters obtained in stage 2 [18] are fixed in this estimation procedure. These parameters include R_a, L_l, L_d, L_q, and a. Then, the parameter vector to be estimated for d-*axis* is $\theta_d = [R_{fd}^* \quad L_{fd} \quad R_{1d} \quad L_{1d}]$ and for q-*axis* is $\theta_q = [R_{1q} \quad L_{1q}]$. The model for estimation can be established as follows:

$$\begin{bmatrix} v_d^* \\ v_{fd} \\ 0 \end{bmatrix} = \begin{bmatrix} -R_a & 0 & 0 \\ 0 & R_{fd} & 0 \\ 0 & 0 & R_{1d} \end{bmatrix} \begin{bmatrix} i_d \\ i_{fd} \\ i_{1d} \end{bmatrix} + \begin{bmatrix} -(L_l + L_{ad}) & \frac{aL_{ad}}{1.5} & L_{ad} \\ -aL_{ad} & \frac{a^2(L_{fd}+L_{ad})}{1.5} & aL_{ad} \\ -L_{ad} & \frac{aL_{ad}}{1.5} & L_{1d} + L_{ad} \end{bmatrix} \cdot p \begin{bmatrix} i_d \\ i_{fd} \\ i_{1d} \end{bmatrix} \tag{5}$$

$$\begin{bmatrix} v_q^* \\ 0 \end{bmatrix} = \begin{bmatrix} -R_a & 0 \\ 0 & R_{1q} \end{bmatrix} \begin{bmatrix} i_q \\ i_{1q} \end{bmatrix} + \begin{bmatrix} -(L_l + L_{aq}) & -L_{aq} \\ -L_{aq} & -(L_l + L_{1q}) \end{bmatrix} p \begin{bmatrix} i_q \\ i_{1q} \end{bmatrix} \tag{6}$$

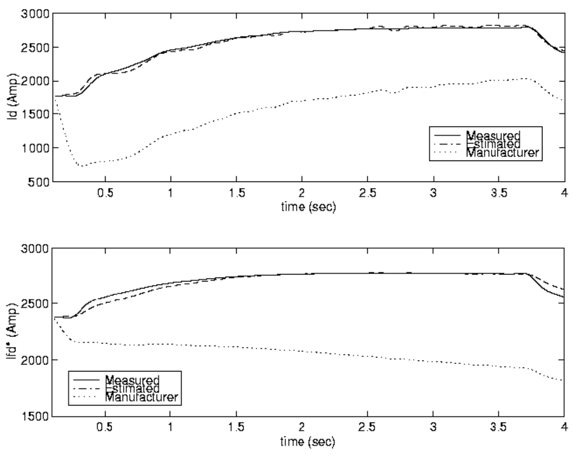

Fig. 5. Test 1: Comparisons of simulated i_d and i^*_{fd} for estimated and manufacturer parameters against measured i_d and i^*_{fd}.

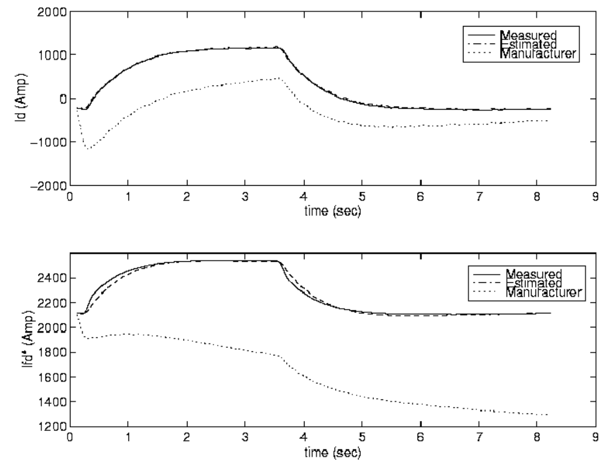

Fig. 6. Test 2: Comparisons of simulated i_d and i^*_{fd} for estimated and manufacturer parameters against measured i_d and i^*_{fd}.

where v^*_d and v^*_q are d- and q-axis voltages as described in Fig. 1 and their computation procedure can be found in [7].

The model (5)–(6) is not in the proper form for estimation. To render them amenable for state space representation, they should be rearranged. This is accomplished by taking current vector i as outputs and voltage vector v as inputs of the system, then the state space form for both models is

$$\dot{i} = -L^{-1}Ri + L^{-1}v. \tag{7}$$

In (5) and (6), i_{1d} and i_{1q} represent unmeasurable rotor body currents for both d- and q-axis. Once the state space estimation models in the form of (7) are obtained, OEM can be employed for the estimation of d- and q-axis rotor body parameters. The estimation algorithm requires initial values for the parameters to be estimated. Manufacturer values are used for this purpose.

In this study, disturbance data were collected at different operating and loading conditions by perturbing the field excitation of the machine or by capturing fault events. A total of such nine disturbance data records were captured and made available for identification. Five of these records include proper large transient dynamics required for the estimation of d- and q-axis damper winding parameters. The remaining four records comprise relatively smaller transient dynamics in that the contribution of damper winding effects are insignificant. However, these records can still be used to estimate field winding parameters R^*_{fd} and L_{fd}. As a result, five sets of d- and q- axis damper winding parameters and nine sets of field winding parameters are estimated using the transient data files provided by APS.

Subsequently, simulation studies are conducted to validate the performance of these estimated parameters. In these studies, the simulated currents generated by using manufacturer and on-line-estimated parameters are compared against corresponding actual measurements. For example, Figs. 5 and 6 illustrate these comparisons for field current i^*_{fd} and d-axis current i_d in two test cases. Validation studies show that estimated rotor body parameters R^*_{fd}, L_{fd} , R_{1d}, and L_{1d} clearly outperform the manufacturer parameters. No appreciable differences were noticed between the performance of estimated R_{1q}, L_{1q}, and manufacturer q-axis rotor body parameters.

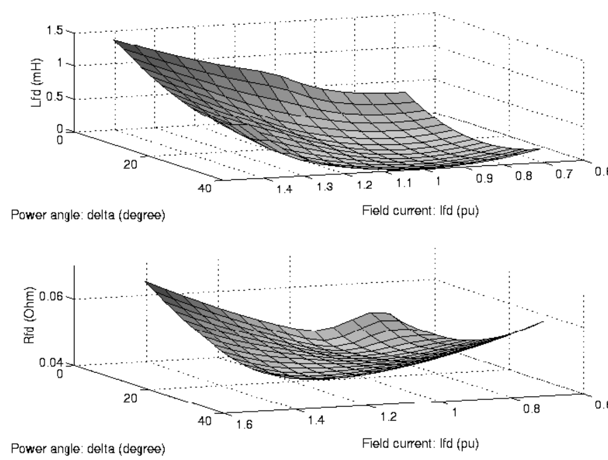

Fig. 7. Variation of L_{fd} and R_{fd} w.r.t. mean power angle (δ) and mean field current (i^*_{fd}).

VI. Development of Rotor Body Models

Using nonlinear mappings [8], the variables representative of generator operating condition are mapped to each rotor body parameter being modeled. Thus, a total of four nonlinear functions are used to model the rotor body parameters R^*_{fd}, L_{fd}, R_{1d}, and L_{1d}.

The generator testing procedure is generally conducted at rated terminal voltage. Hence, the operating region of the generator can be determined by using the field current i^*_{fd} and power angle δ. Due to the fact that the variables i^*_{fd} and δ are not constant during a disturbance, there is not one unique point that can represent each measurement record to be used to develop models of rotor body parameters. Well-known statistical variables, mean value, and standard deviations of i^*_{fd} and δ are used for this purpose.

It is desirable to visualize the transfer functions of rotor body parameters with respect to all variables of input vector space P; however, this can be at most represented in three dimensions. For example, the approximate nonlinear mappings between $E(\boldsymbol{i}^*_{fd})$, $E(\boldsymbol{\delta})$, and operating condition dependent R^*_{fd} and L_{fd} are portrayed in Fig. 7. These three-dimensional (3-D)

TABLE II
COMPARISON OF OEM-ESTIMATED AND NONLINEAR MODEL ESTIMATED PARAMETERS FOR THE CROSS VALIDATION DATA SET

	Data Set #1		*Data Set #2*	
	R_{fd}^* (Ω)	L_{fd} (mH)	R_{1d}^* (Ω)	L_{fd} (mH)
OEM Estimate	0.0460	0.3161	0.0493	0.7160
Nonlinear Estimate	0.0465	0.3260	0.0472	0.7497
% Error	1.07	1.24	4.20	4.71

plots represent the variation manifolds within the bounds of estimated parameter values.

In order to verify that the nonlinear mapping functions are able to generalize properly, cross validation data sets, which are not included in the estimation, are used after the estimation. Table II compares nonlinear model estimated and OEM-estimated d-axis parameters for the data set not used in estimation. As can be seen, nonlinear models can correctly interpolate for the patterns not used in estimation.

Due to the very limited number of data sets available for R_{1d} and L_{1d} estimates, all estimates are used for model estimation and not left for validation procedure.

VII. CONCLUSIONS

A nonlinear mapping-based modeling technique for a large utility generator is developed. Operating data collected online at different levels of excitation and loading conditions are used for estimation. The disturbance data used for estimation are obtained by perturbing the field side of the machine or by capturing fault events. Small excitation disturbance data sets are first used to estimate linear model machine parameters. Subsequently, saturable inductances L_{ds} and L_{qs} are identified for each steady-state operating point based on the estimates of linear model parameters. Nonlinear saturation models are developed by mapping generator terminal variables to L_{ds} and L_{qs} estimates. An OEM technique is later employed to estimate the operating point dependent rotor body parameters. Rotor body models are developed by mapping field current i_{fd}^* and power angle δ to the parameter estimates.

Simulation studies show that estimated parameters clearly outperform the manufacturer parameters. It has also been shown that nonlinear models can correctly interpolate between patterns not used in training. It is expected that a richer data set collected at different loading and excitation levels would improve the performance of such nonlinear mapping models.

ACKNOWLEDGMENT

The authors acknowledge the assistance of J. Demcko of APS.

REFERENCES

[1] *IEEE Guide for Synchronous Generator Modeling Practices in Stability Analysis*, IEEE Std. 1110., 1991.

[2] A. El-Serafi, A. Abdallah, M. El-Sherbiny, and E. Badawy, "Experimental study of the saturation and the cross-magnetizing phenomenon in saturated synchronous machines," *IEEE Trans. Energy Conversion*, vol. 3, pp. 815–823, Dec. 1988.

[3] F. De Mello and L. Hannett, "Representation of saturation in synchronous machines," *IEEE Trans. Power Syst.*, vol. PS-1, pp. 8–14, Nov. 1986.

[4] S. Minnich, R. Schulz, D. Baker, D. Sharma, R. Farmer, and J. Fish, "Saturation functions for synchronous generators from finite elements," *IEEE Trans. Energy Conversion*, vol. EC-2, pp. 680–687, Dec. 1987.

[5] H. Tsai, A. Keyhani, J. A. Demcko, and D. A. Selin, "Development of a neural network saturation model for synchronous generator analysis," *IEEE Trans. Energy Conversion*, vol. 10, pp. 617–624, Dec. 1995.

[6] L. Xu, Z. Zhao, and J. Jiang, "On–line estimation of variable parameters of synchronous machines using a novel adaptive algorithm – Estimation and experimental verification," *IEEE Trans. Energy Conversion*, vol. 12, pp. 200–210, Sept. 1997.

[7] S. Pillutla and A. Keyhani, "Neural network based modeling of round rotor synchronous generator rotor body parameters from operating data," *IEEE Trans. Energy Conversion*, vol. 14, pp. 321–327, Sept. 1999.

[8] ——, "Neural network based saturation model for round rotor synchronous generator," *IEEE Trans. Energy Conversion*, vol. 14, pp. 1019–1025, Dec. 1999.

[9] H. Tsai, A. Keyhani, J. A. Demcko, and R. G. Farmer, "On-line synchronous machine parameter estimation from small disturbance operating data," *IEEE Trans. Energy Conversion*, vol. 10, pp. 25–36, Mar. 1995.

[10] K. S. Narendra and K. Parthasarathy, "Identification and control of dynamical systems using neural networks," *IEEE Trans. Neural Networks*, vol. 1, pp. 4–27, Mar. 1990.

[11] I. M. Canay, "Causes of discrepancies on calculation of rotor quantities and exact equivalent diagrams of the synchronous machine," *IEEE Trans. Power Apparat. Syst.*, vol. PAS-88, pp. 1114–1120, July 1969.

[12] J. L. Kirtley Jr., "On turbine-generator rotor equivalent circuit structures for empirical modeling of turbine generators," *IEEE Trans. Power Syst.*, vol. 9, pp. 269–271, Feb. 1994.

[13] I. Kamwa, P. Viarouge, and J. Dickinson, "Identification of generalized models of synchronous machines from time-domain tests," *Proc. Inst. Elect. Eng.*, pt. C, vol. 138, no. 6, pp. 485–498, Nov. 1991.

[14] S. Salon, "Obtaining synchronous machine parameters from test," in *Proc. Symp. Synchronous Mach. Modeling for Power Syst. Stud.*, Piscataway, NJ, no. 83THO101–6-PWR.

[15] S. R. Chaudhary, S. Ahmed-Zaid, and N. A. Demerdash, "An artificial neural network model for the identification of saturated turbo-generator parameters based on a coupled finite-element/state-space computational algorithm Self-Calibrating power angle instrument," *IEEE Trans. Energy Conversion*, vol. 10, pp. 625–633, Dec. 1995.

[16] J. A. Demcko and J. P. Chrysty, "Self-Calibrating Power Angle Instrument," EPRI, EPRI GS-6475, Res. Project 2591-1, vol. 2, 1989.

[17] M. A. Arjona and D. C. Macdonald, "A new lumped steady-state synchronous machine model derived from finite element analysis," *IEEE Trans. Energy Conversion*, vol. 14, pp. 1–7, Mar. 1999.

[18] H. Karayaka, A. Keyhani, B. Agrawal, D. Selin, and G. Heydt, "Identification of armature, field and saturated parameters of a large steam turbine-generator from operating data," *IEEE Trans. Energy Conversion*, vol. 15, pp. 181–187, June 2000.

[19] M. Hagan and M. B. Menhaj, "Training feedforward networks with the Marquardt algorithm," *IEEE Trans. Neural Networks*, vol. 5, pp. 989–993, Nov. 1994.

[20] H. Tsai, A. Keyhani, J. A. Demcko, and R. G. Farmer, "On-line synchronous machine parameter estimation from small disturbance operating data," *IEEE Trans. Energy Conversion*, vol. 10, pp. 25–36, Mar. 1995.

[21] H. Karayaka, A. Keyhani, B. Agrawal, D. Selin, and G. Heydt, "Methodology development for estimation of armature circuit and field winding parameters of large utility generators," *IEEE Trans. Energy Conversion*, vol. 14, pp. 901–908, Dec. 1999.

H. Bora Karayaka received the B.S.E.E. and M.S.E.E. degrees from Istanbul Technical University, Istanbul, Turkey, in 1987 and 1990, respectively. He is currently pursuing the Ph.D. degree in the Department of Electrical Engineering at The Ohio State University, Columbus.

He is a Research Associate at The Ohio State University.

Ali Keyhani (S'69–M'72–S'72–M'76–SM'89–F'98) received the Ph.D. degree from Purdue University, West Lafayette, IN, in 1975.

Currently, he is a Professor of electrical engineering at The Ohio State University, Columbus. His research interests include control and modeling, parameter estimation, failure detection of electric machines, transformers, and drive systems.

Gerald Thomas Heydt (S'62–M'71–SM'79–F'91) received the B.E.E.E. degree from the Cooper Union College, New York, and the M.S.E.E. and Ph.D. degrees from Purdue University, West Lafayette, IN.

Currently, he is a Professor of Electrical Engineering at Arizona State University, Tempe.

Baj L. Agrawal (S'74–M'74–SM'83–F'94) received the B.S. degree in electrical engineering from Birla Institute of Technology and Science, Birla, India, in 1970, and the M.Sc. and Ph.D. degrees from the University of Arizona, Tucson.

Currently, he is a Senior Consulting Engineer with Arizona Public Service Company, Phoenix, where he has been since 1974.

Douglas A. Selin (M'85–SM'00) received the B.S.E.E. degree from Brigham Young University, Provo, UT, in 1983, and the M.Eng. degree from Rensselaer Polytechnic Institute, Troy, NY, in 1984.

Currently, he is with Arizona Public Service Company, Phoenix, where his responsibilities include subsynchronous resonance problem analysis and simulation of power system dynamics and transients.